**Jurnal Farmasi Ma Chung: Sains Teknologi dan Klinis Komunitas**

***p–ISSN :*** **2986-8270**
***e-ISSN :*** **2986-5972**
**DOI: 10.33479/jfmc.v4i2.187**
Research Article

# Optimized Resveratrol-Loaded SNEDDS Gel Enhances Antioxidant Activity and In Vitro Release

**Article History:**
Accepted: 28 August 2026
Revised: 27 October 2026
Published: 02 November 2026

**Keywords:**
*Antioxidant Gel;*
*D-optimal Mixture Design;*
*Franz Diffusion;*
*Resveratrol;*
*SNEDDS*

**Shella Pradina Utami[1*], Ilham Kuncahyo[2], Nuraini Harmastuti[3]**

Resveratrol is a potent polyphenolic antioxidant with poor aqueous solubility and light sensitivity, which limit its topical application. This study developed and optimized a resveratrol self-nanoemulsifying drug delivery system (SNEDDS), incorporated the optimized system into a gel, and compared its physical characteristics, antioxidant activity, and in vitro release with those of a conventional resveratrol gel. A 16-run D-optimal mixture design was employed using virgin coconut oil (10–20%), Tween 80 (50–80%), and polyethylene glycol 400 (10–30%) as the oil, surfactant, and co-surfactant. The optimized composition consisted of 13.8131% virgin coconut oil, 61.7834% Tween 80, and 24.4036% polyethylene glycol 400, with a desirability value of 0.829. Experimental verification yielded a droplet size of 15.23 nm, emulsification time of 8.12 s, transmittance of 99.63%, drug loading of 46.51 mg/mL, polydispersity index of 0.157, and zeta potential of −11.77 mV, with no significant differences from the predicted values ($p>0.05$). The optimized SNEDDS gel exhibited good homogeneity and physical stability. DPPH radical-scavenging activity was stronger for the SNEDDS gel than for the conventional resveratrol gel, with $IC_{50}$ values of 7.25±0.02 and 9.01±0.03 µg/mL and antioxidant activity indices of 5.45±0.012 and 4.38±0.013, respectively. At 120 min, cumulative resveratrol release reached 155.28 µg/cm² (62.11%) for the SNEDDS gel compared with 134.35 µg/cm² (53.74%) for the conventional gel, representing a 15.6% higher release ($p=0.046$). Overall, the optimized SNEDDS gel enhanced antioxidant activity and in vitro release, demonstrating potential for improved topical resveratrol delivery.

**Copyright:** © 2023 by the authors. Submitted for possible open access publication under the terms and conditions of the Creative Commons Attribution (CC BY) license (https://creativecommons.org/licenses/by/4.0/).

The skin is the body's largest organ and its primary interface with the external environment. Its stratified epidermis, dermis, and subcutaneous tissue jointly provide physical, chemical, immunological, sensory, and thermoregulatory protection while limiting transepidermal water loss and the entry of potentially harmful agents [1]. Because this barrier is continuously exposed to solar radiation, pollution, and oxidants, maintaining its structural and biochemical integrity is essential for cutaneous homeostasis.

Photoaging is the premature, extrinsic ageing of skin caused mainly by repeated ultraviolet exposure. Ultraviolet radiation increases reactive oxygen species, activates matrix metalloproteinases, and accelerates collagen and elastin degradation, producing wrinkles, pigmentary changes, dryness, loss of elasticity, and chronic inflammation [2,3].

[1,2,3] Master of Pharmacy Study Program, Faculty of Pharmacy, Universitas Setia Budi, Surakarta, Indonesia

Email: shellapradina7@gmail.com

When endogenous antioxidant defences are insufficient to compensate for sustained oxidative stress, topical antioxidants can help neutralize radicals near the site of exposure and complement photoprotection.

Resveratrol (3,5,4'-trihydroxystilbene) is a naturally occurring stilbene polyphenol with direct radical-scavenging, anti-inflammatory, and photoprotective activities that support its development as an anti-ageing active [4]. Its three phenolic hydroxyl groups donate hydrogen or electrons and help modulate endogenous antioxidant pathways. However, resveratrol has very low aqueous solubility (<0.05 mg/mL), high permeability, and therefore Biopharmaceutics Classification System class II behaviour; it is also photosensitive and susceptible to trans-to-cis isomerization and oxidative degradation [5,6]. These properties hinder uniform dispersion, release, and effective topical delivery from conventional hydrophilic vehicles.

A self-nanoemulsifying drug delivery system (SNEDDS) can address these limitations by dissolving a lipophilic active in an isotropic mixture of oil, surfactant, and co-surfactant that spontaneously forms a fine oil-in-water nanoemulsion on dilution [7]. Nanometre-scale droplets increase interfacial area, maintain resveratrol in a solubilized state, and can improve wetting, release, and contact with the skin surface. Incorporation of the optimized liquid system into a hydrogel further improves handling, application, and residence time while retaining the solubilization advantage [8].

Because the total proportion of the oil, surfactant, and co-surfactant must equal 100%, their effects cannot be optimized independently. D-optimal mixture design efficiently selects informative compositions within constrained component ranges and estimates both individual and interaction effects with fewer experimental runs than exhaustive testing [9]. Here, virgin coconut oil (VCO), Tween 80, and polyethylene glycol (PEG) 400 were selected as the oil, surfactant, and co-surfactant, respectively, and six quality responses were optimized simultaneously.

Although resveratrol SNEDDS formulations and their physicochemical optimization have been reported [10-12], many studies remain focused on preconcentrate characterization or non-topical applications. Studies that progress from an optimized SNEDDS to a topical gel and directly compare it with a conventional gel in both radical-scavenging capacity and in vitro release remain limited [13,14]. Accordingly, this study had four objectives: (1) determine how the VCO-Tween 80-PEG 400 proportions affect droplet size, emulsification time, transmittance, drug loading, polydispersity index, and zeta potential; (2) obtain and verify an optimum SNEDDS using D-optimal mixture design; (3) compare resveratrol release from the SNEDDS and conventional gels using a Franz diffusion cell; and (4) compare their DPPH radical-scavenging activities using $IC_{50}$ and the antioxidant activity index.

## Results and Discussion

### Identity of the Resveratrol Raw Material and Validation of the Analytical Method

The FTIR spectrum of the raw material showed the characteristic functional groups of trans-resveratrol. The principal bands occurred at 3190 $cm^{-1}$ (phenolic O-H stretching), 1585 and 1512 $cm^{-1}$ (aromatic C=C stretching), 1444 $cm^{-1}$ (aromatic skeletal vibration), 1147 $cm^{-1}$ (phenolic C-O stretching), 966 $cm^{-1}$ (trans HC=CH), and 831 $cm^{-1}$ (out-of-plane aromatic C-H). These bands corresponded closely to the literature values reported in the thesis (3422, 1587, 1512, 1443, 1153, 965, and 831 $cm^{-1}$, respectively), with no new or missing characteristic peaks. The small shifts were within the range attributable to instrument, pellet preparation, and intermolecular interactions, confirming the identity and structural integrity of the resveratrol raw material [4,15].

The UV-Vis method was specific at 306 nm because the placebo containing the SNEDDS components and gel base showed no interfering absorption. The calibration relationship over 2-10 µg/mL was $y = 0.0237x + 0.3068$ ($R^2 = 0.999$). Mean recovery was 100.27%, repeatability at 6 µg/mL gave an RSD of 0.16%, and the limits of detection and quantification

were 0.111 and 0.338 µg/mL, respectively. These findings satisfied the acceptance criteria applied in the thesis and supported the use of the method for drug-loading and release measurements [16,17].

### Effect of the Component Ratio on SNEDDS Characteristics

Sixteen formulations were generated by the D-optimal mixture design within the constrained ranges of VCO 10-20%, Tween 80 50-80%, and PEG 400 10-30%. The wide response ranges - droplet size 14.01-286.20 nm, emulsification time 4.62-19.78 s, transmittance 87.49-99.98%, drug loading 42.81-49.08 mg/mL, PDI 0.1027-0.4918, and zeta potential -7.35 to -18.95 mV - demonstrate that SNEDDS quality depended on component balance rather than on absolute amounts alone (Table 1).

**Table 1.** D-optimal mixture-design compositions and experimental SNEDDS responses

| Run | VCO (%) | Tween 80 (%) | PEG 400 (%) | Droplet size (nm) | Emulsification time (s) | Transmittance (%) | Drug loading (mg/mL) | PDI | Zeta potential (mV) |
|---|---|---|---|---|---|---|---|---|---|
| 1 | 15.8927 | 68.0437 | 16.0636 | 27.67 | 8.86 | 99.39 | 45.46 | 0.177 | -11.72 |
| 2 | 19.2371 | 70.7629 | 10 | 170.16 | 10.69 | 94.16 | 44.80 | 0.3613 | -16.54 |
| 3 | 14.7357 | 63.2945 | 21.9698 | 24.77 | 8.95 | 99.52 | 46.57 | 0.1472 | -11.86 |
| 4 | 10.8501 | 74.2232 | 14.9268 | 20.08 | 5.43 | 99.75 | 43.59 | 0.1235 | -7.84 |
| 5 | 20 | 60.73 | 19.27 | 286.20 | 19.78 | 87.49 | 47.17 | 0.4918 | -17.94 |
| 6 | 10 | 80 | 10 | 30.37 | 4.62 | 99.06 | 42.81 | 0.2074 | -7.35 |
| 7 | 10 | 60 | 30 | 21.96 | 6.68 | 99.64 | 47.93 | 0.1423 | -12.93 |
| 8 | 14.9514 | 55.0486 | 30 | 44.27 | 10.21 | 98.97 | 48.64 | 0.2543 | -13.74 |
| 9 | 19.2371 | 60 | 20,7629 | 195.30 | 13.43 | 92.21 | 48.59 | 0.399 | -10.88 |
| 10 | 10 | 69.2519 | 20.7481 | 14.01 | 6.09 | 99.98 | 46.59 | 0.1027 | -8.16 |
| 11 | 14.9514 | 55.0486 | 30 | 43.61 | 10.71 | 98.03 | 48.62 | 0.251 | -13.58 |
| 12 | 10 | 80 | 10 | 32.30 | 4.92 | 98.94 | 43.12 | 0.2134 | -7.48 |
| 13 | 19.2371 | 70.7629 | 10 | 172.04 | 11.26 | 94.17 | 44.61 | 0.3667 | -16.41 |
| 14 | 20 | 55.4607 | 24.5393 | 281.35 | 19.30 | 88.86 | 48.91 | 0.4882 | -18.46 |
| 15 | 20 | 50 | 30 | 265.90 | 18.81 | 90.92 | 48.99 | 0.4655 | -18.79 |
| 16 | 20 | 50 | 30 | 271.70 | 18.95 | 90.13 | 49.08 | 0.47 | -18.95 |

The selected models were quadratic for droplet size, emulsification time, transmittance, and zeta potential, and special cubic for drug loading and PDI. With A, B, and C denoting the proportions of VCO, Tween 80, and PEG 400, respectively, the fitted equations were:

$Y_1$ (droplet size, nm) = 4096.92A + 22.04B + 133.48C - 5137.94AB - 5284.69AC + 2.25BC

$Y_2$ (emulsification time, s) = 132.99A + 4.08B + 8.26C - 150.56AB - 136.19AC + 11.80BC

$Y_3$ (transmittance, %) = -65.78A + 99.73B + 96.51C + 209.61AB + 212.20AC - 5.05BC

$Y_4$ (drug loading, mg/mL) = -322.42A + 42.99B + 44.75C + 674.93AB + 676.59AC + 15.47BC - 705.33ABC + 361.63AB(A-B) + 318.91AC(A-C) - 9.04BC(B-C)

$Y_5$ (PDI) = 5.54A + 0.2133B + 0.6760C - 6.99AB - 8.24AC - 1.15BC + 4.49ABC

$Y_6$ (zeta potential, mV) = -80.47A - 7.21B - 16.55C + 61.75AB + 84.43AC + 7.60BC

**Table 2.** Fit statistics for the six SNEDDS response models

| Response | Model | F | p | Lack of fit (p) | $R^2$ | Adjusted $R^2$ | Predicted $R^2$ | Adeq. precision |
|---|---|---|---|---|---|---|---|---|
| Droplet size | Quadratic | 17.06 | 0.0001 | 0.9015 | 0.8951 | 0.8426 | 0.6839 | 9.8823 |
| Emulsification time | Quadratic | 21.91 | <0.0001 | 0.7179 | 0.9164 | 0.8745 | 0.7538 | 13.2368 |
| Transmittance | Quadratic | 11.13 | 0.0008 | 0.6948 | 0.8477 | 0.7715 | 0.5553 | 7.7575 |
| Drug loading | Special cubic | 119.63 | <0.0001 | 0.1928 | 0.9945 | 0.9861 | 0.9662 | 29.2021 |
| PDI | Special cubic | 11.86 | 0.0008 | 0.9986 | 0.8877 | 0.8128 | 0.6385 | 9.4689 |
| Zeta potential | Quadratic | 162.14 | <0.0001 | 0.7574 | 0.9878 | 0.9817 | 0.9645 | 34.0613 |

Table 2 summarizes the statistical adequacy of the models selected to describe the effects of VCO, Tween 80, and PEG 400 proportions on the six SNEDDS responses. Quadratic models were selected for droplet size, emulsification time, transmittance, and zeta potential, whereas special-cubic models were required for drug loading and PDI. The selection of quadratic and special-cubic models indicates that the SNEDDS characteristics were influenced not only by the individual proportions of the three components but also by interactions among them. All models were statistically significant, with model p-values ranging from <0.0001 to 0.0008. Therefore, the variations observed in the responses were unlikely to have resulted from random experimental error.

The lack-of-fit p-values ranged from 0.1928 to 0.9986 and were greater than 0.05 for all responses. A non-significant lack of fit indicates that the differences between the experimental results and the values estimated by the models were not significantly greater than the pure experimental error. Thus, the selected models adequately represented the experimental data within the investigated mixture-design space. In addition, the adequate-precision values ranged from 7.7575 to 34.0613, exceeding the minimum signal-to-noise ratio of 4. These results demonstrate that all models provided sufficient signals to navigate the specified ranges of VCO, Tween 80, and PEG 400.

The quadratic droplet-size model was significant ($F = 17.06$; $p = 0.0001$) and explained 89.51% of the observed variability ($R^2 = 0.8951$). Its adjusted $R^2$ of 0.8426 and predicted $R^2$ of 0.6839 indicated satisfactory agreement between the descriptive and predictive capacities of the model. The adequate-precision value of 9.8823 further confirmed that the model had a sufficient signal for evaluating the effects of the component proportions on droplet size. Similarly, the emulsification-time model showed a significant quadratic relationship ($F = 21.91$; $p < 0.0001$), with $R^2$, adjusted $R^2$, and predicted $R^2$ values of 0.9164, 0.8745, and 0.7538, respectively. These results indicate that the model explained most of the variation in emulsification time and retained satisfactory predictive capability within the experimental region.

The transmittance model was also significant ($F = 11.13$; $p = 0.0008$), with an $R^2$ of 0.8477. However, the adjusted $R^2$ of 0.7715 and predicted $R^2$ of 0.5553 showed a greater difference than those obtained for droplet size and emulsification time. This suggests that the model was adequate for describing the experimental trend but had comparatively lower predictive strength. Nevertheless, its non-significant lack of fit ($p = 0.6948$) and adequate-precision value of 7.7575 supported its use for interpreting transmittance within the studied component ranges.

Drug loading required a special-cubic model and produced a high model F-value of 119.63 with $p < 0.0001$. The model showed an excellent descriptive fit, as indicated by its $R^2$ of 0.9945 and adjusted $R^2$ of 0.9861. Its non-significant lack of fit ($p = 0.1928$) and high adequate-precision value of 29.2021 also demonstrated a strong signal within the experimental design. Moreover, the predicted $R^2$ was high (0.9662), indicating that the model had excellent predictive capability and could reliably predict new observations within the investigated design space. The close agreement between the adjusted and predicted $R^2$ values further supported the model's robustness and predictive reliability. This strong model performance may be attributed to the ability of the special-cubic model to adequately describe the response across the constrained mixture region. Therefore, the drug-loading model was considered suitable for describing and predicting the response within the investigated design space. Experimental verification of the optimum formulation was consequently essential to confirm the predicted drug-loading value.

The special-cubic PDI model was significant ($F = 11.86$; $p = 0.0008$), with an $R^2$ of 0.8877, adjusted $R^2$ of 0.8128, and predicted $R^2$ of 0.6385. The relatively close adjusted and predicted $R^2$ values indicated satisfactory predictive consistency, while the lack-of-fit p-value of 0.9986 showed a very good agreement between the fitted model and experimental observations. Its adequate-precision value of 9.4689

also confirmed that the model could be used to navigate the design space.

Among the six responses, the quadratic zeta-potential model exhibited the strongest overall statistical performance. It produced the highest F-value of 162.14 with $p < 0.0001$ and explained 98.78% of the observed variability ($R^2 = 0.9878$). The adjusted $R^2$ of 0.9817 and predicted $R^2$ of 0.9645 were very close, demonstrating excellent agreement between model fitting and prediction. The non-significant lack of fit ($p = 0.7574$) and the highest adequate-precision value of 34.0613 further confirmed the robustness of this model. Overall, the statistical results support the use of the selected models for simultaneous SNEDDS optimization, although predictions for drug loading require greater caution and confirmation through experimental verification.

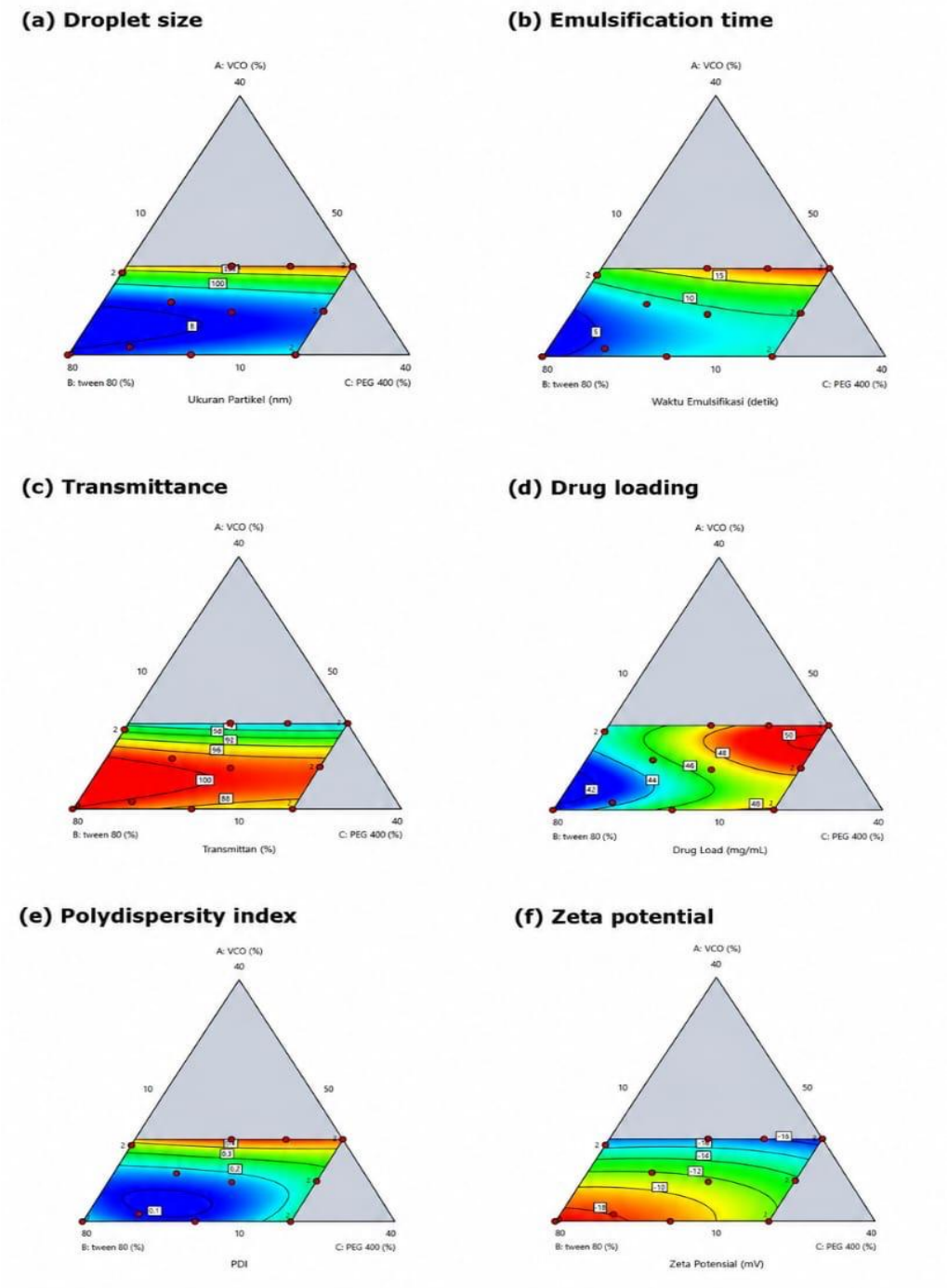



**Figure 1.** Contour plots of the D-optimal mixture design for (a) droplet size, (b) emulsification time, (c) transmittance, (d) drug loading, (e) PDI, and (f) zeta potential. A = VCO, B = Tween 80, and C = PEG 400.

The equations and contour plots (Figure 1) consistently show that VCO was the principal driver of larger droplets, longer emulsification times, and broader size distributions when its proportion increased without a proportional increase in interfacial stabilizers. Tween 80 lowered interfacial tension, whereas PEG 400 increased interfacial flexibility; their balance with VCO produced smaller, faster-forming, and more uniform droplets [7,18,19]. Consequently, the smallest droplets, shortest emulsification times, highest clarity, and lowest PDI were found in the lower-VCO, higher-Tween 80 region.

Transmittance decreased with increasing VCO and increased with Tween 80 and PEG 400, consistent with reduced light scattering by finer and more uniform droplets. Drug loading followed the more complex special-cubic model: the highest loading occurred toward higher PEG 400 with low-to-moderate VCO and intermediate Tween 80, emphasizing that solubilization was governed by interactions among components rather than by oil content alone. Zeta potential ranged from -7.35 to -18.95 mV. Because Tween 80 and PEG 400 are non-ionic, stability was not expected to rely solely on large electrostatic potentials; steric protection of the droplet interface also contributes substantially [18,20].

**Determination and Verification of the Optimum Formulation**

Numerical optimization minimized droplet size, emulsification time, and PDI, maximized transmittance and drug loading, and retained zeta potential within the observed range. The best compromise contained 13.8131% VCO, 61.7834% Tween 80, and 24.4036% PEG 400, with an overall desirability of 0.829 (Figure 2). This surfactant-rich but balanced composition was consistent with the response surfaces: sufficient Tween 80 promoted rapid formation of clear nanodroplets, while PEG 400 supported interfacial flexibility and resveratrol solubilization [9].

Table 3 shows that the optimum SNEDDS formulation consisted of 13.8131% VCO, 61.7834% Tween 80, and 24.4036% PEG 400, with a desirability value of 0.829. This formulation produced a small droplet size of 15.23 nm, rapid emulsification time of 8.12 s, high transmittance of 99.63%, drug loading of 46.51 mg/mL, a low PDI of 0.157, and a zeta potential of −11.77 mV. The verification results showed no significant differences between the predicted and experimental values for all responses ($p>0.05$), demonstrating that the D-optimal model successfully identified a reproducible optimum formulation within the investigated component ranges

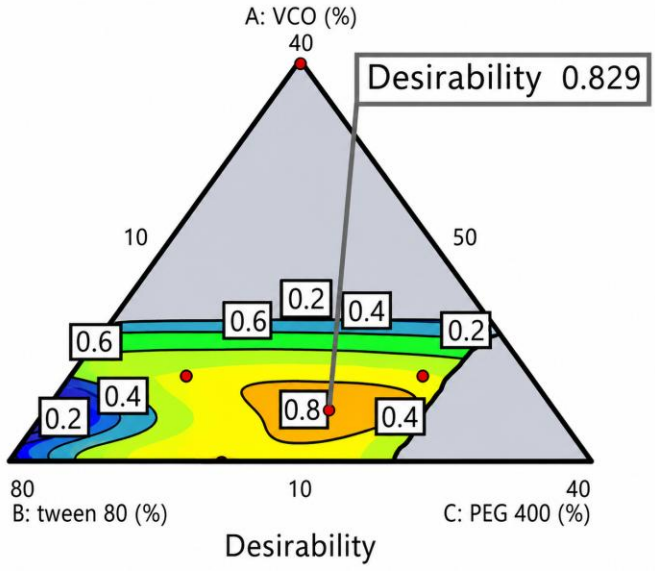



**Figure 2.** D-optimal desirability contour plot for simultaneous optimization of the six SNEDDS responses. A = VCO, B = Tween 80, and C = PEG 400.

**Table 3.** Composition, experimental characteristics, and verification of the optimum resveratrol SNEDDS

| Parameter | Optimum/observed value | Verification p-value |
|---|---|---|
| VCO (%) | 13.8131 | - |
| Tween 80 (%) | 61.7834 | - |
| PEG 400 (%) | 24.4036 | - |
| Desirability | 0.829 | - |
| Droplet size (nm) | 15.23 | 0.400 |
| Emulsification time (s) | 8.12 | 0.532 |
| Transmittance (%) | 99.63 | 1.000 |
| Drug loading (mg/mL) | 46.51 | 0.518 |
| PDI | 0.157 | 0.537 |
| Zeta potential (mV) | -11.77 | 0.598 |

**Physical Quality of the Gels**

Table 4 demonstrates that both formulations were initially odorless, smooth, and clear; however, the SNEDDS gel showed better homogeneity than the conventional gel. The SNEDDS gel also had lower viscosity and adhesion but greater spreadability at all applied loads, indicating that it was easier to distribute across the application surface. After six cycling-test cycles, the conventional gel became slightly turbid and remained less homogeneous, whereas the SNEDDS gel retained its clear and homogeneous appearance. Although both formulations showed slight changes in pH and viscosity, the overall observations indicate that the SNEDDS gel maintained its physical characteristics better during the cycling test.

**Table 4.** Physical quality and cycling-test results of the conventional and SNEDDS resveratrol gels

| Parameter | Conventional resveratrol gel | Resveratrol SNEDDS gel |
|---|---|---|
| Appearance | Odorless, smooth, clear | Odorless, smooth, clear |
| Homogeneity | Less homogeneous | Homogeneous |
| pH | 5.76 ± 0.03 | 5.33 ± 0.08 |
| Viscosity (cP) | 4465 ± 37.51 | 2976 ± 38.28 |
| Adhesion (s) | 5.47 ± 0.08 | 4.21 ± 0.04 |
| Spread, 50 g (cm) | 4.17 ± 0.21 | 4.63 ± 0.15 |
| Spread, 100 g (cm) | 5.37 ± 0.06 | 5.57 ± 0.06 |
| Spread, 150 g (cm) | 5.67 ± 0.06 | 6.10 ± 0.10 |
| After 6 cycling-test cycles | Odorless, smooth, slightly turbid, less homogeneous | Odorless, smooth, clear, homogeneous |
| pH after cycle 6 | 5.42 ± 0.04 | 5.28 ± 0.01 |
| Viscosity after cycle 6 (cP) | 4715 ± 93.55 | 3271 ± 93.12 |

**Antioxidant Activity**

Both gels were odorless, smooth, and clear, but the conventional gel was less homogeneous because poorly water-soluble resveratrol remained incompletely dispersed. In the SNEDDS gel, resveratrol was already solubilized within nanodroplets and more uniformly through the HPMC matrix. The pH values remained within the topical range applied in the thesis, while the lower viscosity of the SNEDDS gel was consistent with the fluid contributions of Tween 80 and PEG 400. Its adhesion remained above the 4-s criterion, and its greater spreadability supported easier distribution over the skin [21,22].

Independent-samples testing showed differences between the gels in pH, viscosity, and adhesion (all $p<0.001$) and in spreadability ($p=0.035$). These statistical differences did not indicate physical failure: both formulations remained within the stated suitability ranges. After six alternating-temperature cycles, the SNEDDS gel remained clear and homogeneous, whereas the conventional gel became slightly turbid. The modest changes in pH and viscosity did not cause phase separation, supporting the superior physical robustness of the solubilized system under the study conditions [23].

The gel base showed only weak activity by AAI, whereas both resveratrol-containing gels were very strong antioxidants (Table 5). One-way ANOVA found significant differences among all three groups for $IC_{50}$ and AAI (both $p<0.001$), and Tukey analysis separated the SNEDDS gel, conventional gel, and base. Relative to the conventional gel, the SNEDDS gel reduced $IC_{50}$ by approximately 19.5% and increased AAI from 4.38 to 5.45. The improvement is consistent with molecular solubilization of resveratrol and its more uniform availability to interact with DPPH; in the conventional gel, undissolved material can limit access to the phenolic hydroxyl groups responsible for hydrogen- or electron-donation [24,25].

In Vitro Release Across a Synthetic Membrane

Cumulative release increased throughout 120 min for both formulations, but the SNEDDS gel was consistently higher at every sampling point (Figure 3). At 120 min, the amount released was approximately 155.28 µg/cm² from the SNEDDS gel and 134.35 µg/cm² from the conventional gel, representing an improvement of about 15.6%. The corresponding percentages were 62.11% and 53.74%, and the difference in percentage release was significant by Mann-Whitney testing ($p=0.046$).

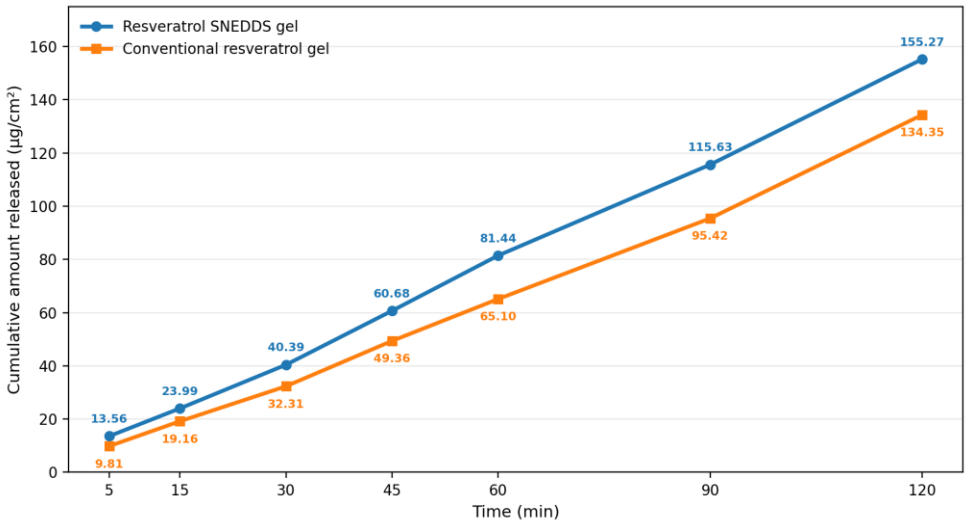



**Figure 3.** Cumulative resveratrol released from the SNEDDS gel and conventional gel across an HT-Tuffryn synthetic membrane into phosphate buffer pH 7.4 at 37 ± 1 °C. Values are mean cumulative amounts from the thesis diffusion dataset.

The higher release from the SNEDDS gel can be explained by the larger interfacial area of its nanodroplets and maintenance of resveratrol in a dissolved state, which sustain the concentration gradient at the donor-membrane interface. Tween 80 and PEG 400 also improve wetting and reduce resistance to mass transfer [11,26]. The HT-Tuffryn membrane provides a controlled formulation-comparison model rather than a biological skin barrier; therefore, the result supports improved in vitro availability but should be confirmed in future studies using skin models, irritation assessment, and in vivo efficacy testing [27].

**Table 5.** DPPH radical-scavenging activity of the gel base and resveratrol gels

| Sample | $IC_{50}$ (µg/mL) | $IC_{50}$ category | AAI | AAI category |
|---|---|---|---|---|
| Gel base | 118.82 ± 0.50 | Moderate | 0.33 ± 0.001 | Weak |
| Conventional resveratrol gel | 9.01 ± 0.03 | Very strong | 4.38 ± 0.013 | Very strong |
| Resveratrol SNEDDS gel | 7.25 ± 0.02 | Very strong | 5.45 ± 0.012 | Very strong |

## Conclusion

The D-optimal mixture design identified a reproducible resveratrol SNEDDS containing 13.8131% VCO, 61.7834% Tween 80, and 24.4036% PEG 400, with a desirability of 0.829 and verified nanometre-scale characteristics. Incorporation into an HPMC gel produced a homogeneous, physically stable topical formulation. Compared with the conventional resveratrol gel, the SNEDDS gel showed stronger DPPH radical-scavenging activity and greater cumulative in vitro release across the synthetic membrane. These findings answer the four study objectives and demonstrate that optimizing the oil-surfactant-co-surfactant balance can improve resveratrol solubilization, formulation uniformity, antioxidant performance, and release from a topical gel. Biological skin-permeation, irritation, and efficacy studies remain necessary before clinical application.

## Materials and Methods

Resveratrol (Tokyo Chemical Industry), VCO, Tween 80, PEG 400, HPMC, propylene glycol, glycerin, methylparaben, propylparaben, DPPH, analytical-grade methanol and ethanol, phosphate buffer, and distilled water were used. Instruments included an FTIR spectrophotometer, Shimadzu UV-1800 UV-Vis spectrophotometer, HORIBA Nano Partica SZ-100 particle-size/zeta-potential analyzer, Mettler Toledo XS205 analytical balance, magnetic stirrer, vortex mixer, ultrasonicator, centrifuge, Brookfield viscometer, pH meter, adhesion and spreadability apparatus, and Franz diffusion cell.

### Identification of resveratrol by infrared spectroscopy

Resveratrol (5 mg) and KBr (500 mg) were homogenized and compressed into a transparent pellet at 2 ton·$cm^{-2}$. The spectrum was recorded from 400 to 4000 $cm^{-1}$ with 400 scans at 4 $cm^{-1}$ resolution, using a KBr pellet as the background. Characteristic functional-group bands were interpreted and compared with the thesis literature reference [15].

### Calibration curve and validation of the analytical method

A 100 µg/mL resveratrol stock solution was prepared in methanol. A 10 µg/mL solution was scanned from 200 to 400 nm, and 306 nm was selected as the analytical wavelength; absorbance stability was evaluated from 0 to 60 min. Calibration standards of 2, 4, 6, 8, and 10 µg/mL were measured at 306 nm. Validation included placebo specificity, linearity, accuracy at 4, 6, and 8 µg/mL in triplicate, repeatability at 6 µg/mL in six replicates, and calculation of LOD and LOQ from the calibration slope and response variation [16,17,28].

### Experimental design

A 16-run D-optimal mixture design was generated in Design-Expert version 13. The independent mixture components were VCO (10-20%), Tween 80 (50-80%), and PEG 400 (10-30%), with their proportions constrained to sum to 100%. The responses were droplet size, emulsification time, transmittance, drug loading, PDI, and zeta potential. Replicated design points were included to estimate experimental error [9].

### Preparation of the resveratrol SNEDDS

For each run, VCO, Tween 80, and PEG 400 were combined according to the design to a total volume of 3 mL. Resveratrol was added progressively to saturation, and the mixture was stirred at 500 rpm for 10 min, sonicated for 10 min, and centrifuged at 5000 rpm for 15 min. The clear supernatant was collected and stored at room temperature before characterization [29].

**Characterisation of the SNEDDS**

For droplet size and PDI, 0.1 mL SNEDDS was diluted with 10 mL distilled water and measured by dynamic light scattering. Zeta potential was determined from the same dilution. Emulsification time was measured after adding 0.1 mL SNEDDS to 10 mL water at 37 ± 1 °C under 500 rpm stirring. The dispersion was stirred for a further 5 min and transmittance was measured at 650 nm. Drug loading was determined by diluting 0.1 mL SNEDDS to 10 mL with methanol and quantifying resveratrol at 306 nm.

**Determination and verification of the optimum formulation**

Response values were fitted in Design-Expert and combined by numerical desirability. Droplet size, emulsification time, and PDI were minimized; transmittance and drug loading were maximized; zeta potential was retained within the observed range. The highest-desirability composition was prepared in triplicate and all six responses were remeasured. Experimental values were compared with predicted values by one-sample t-tests.

**Preparation of the gels**

The conventional formulation contained 0.2% resveratrol, 2% HPMC, 15% propylene glycol, 10% glycerin, 0.02% methylparaben, 0.01% propylparaben, and water to 100%. The SNEDDS gel used 0.2% resveratrol-loaded optimum SNEDDS with the same gel base. HPMC was dispersed in water at 80-90 °C and allowed to hydrate. Parabens were dissolved in propylene glycol, glycerin and the respective active phase were added, and this mixture was incorporated gradually into the hydrated HPMC before adjustment to final mass with water [21].

**Evaluation of physical quality**

Appearance, odor, texture, and homogeneity were inspected visually. pH was measured with a calibrated meter. Viscosity was determined using a Brookfield viscometer at 50 rpm. Adhesion was measured with 0.5 g gel between glass slides after a 50-g preload, and spreadability was measured with 0.5 g gel after 50-, 100-, and 150-g loads. Physical stability was assessed over six 24-h cycles alternating between 5 and 35 °C, after which appearance, homogeneity, pH, and viscosity were reassessed [22,30].

**DPPH radical-scavenging assay**

DPPH stock solution (0.2 mM) was prepared by dissolving 19.7 mg DPPH in methanol to 250 mL and protecting it from light. Each gel sample was prepared as a 100 µg/mL stock and diluted to 2, 4, 6, 8, and 10 µg/mL. One millilitre of each dilution was mixed with 1 mL DPPH solution, incubated in the dark for 30 min, and measured at 517 nm. Inhibition was calculated against the DPPH control, $IC_{50}$ was estimated from linear regression, and AAI was calculated as the final DPPH concentration (39.5 µg/mL) divided by $IC_{50}$ [31,32].

**In vitro release using a Franz diffusion cell**

Resveratrol release was measured across an HT-Tuffryn synthetic membrane in a Franz diffusion cell. Gel (0.25 g) was spread on the donor-facing membrane surface, and the receptor compartment contained 25 mL phosphate buffer pH 7.4 maintained at 37 ± 1 °C with continuous stirring. Samples (5 mL) were collected at 5, 15, 30, 45, 60, 90, and 120 min and quantified by UV-Vis spectrophotometry at 306 nm [27].

**Data analysis**

The 16-run response data were analysed by ANOVA in Design-Expert version 13; model significance and lack of fit were evaluated, and the optimum was selected by the highest desirability. Verification used one-sample t-tests in SPSS version 25. Between-formulation comparisons used independent-samples t-tests for normally distributed data or Mann-Whitney tests otherwise. One-way ANOVA with Tukey post-hoc analysis was used for antioxidant comparisons. The significance threshold was 0.05.

**References**

1. Baker P, Huang C, Radi R, Moll SB, Jules E, Arbiser JL. Skin barrier function: the interplay of physical, chemical, and immunologic properties. Cells. 2023;12(23). doi:10.3390/cells12232745.

2. Calvo MJ, Navarro C, Durán P, et al. Antioxidants in photoaging: from molecular insights to clinical applications. Int J Mol Sci. 2024;25(4). doi:10.3390/ijms25042403.

3. Naharro-Rodriguez J, Bacci S, Hernandez-Bule ML, Perez-Gonzalez A, Fernandez-Guarino M. Decoding skin aging: a review of mechanisms, markers, and modern therapies. Cosmetics. 2025;12(4). doi:10.3390/cosmetics12040144.

4. Rosiak N, Cielecka-Piontek J, Skibiński R, Lewandowska K, Bednarski W, Zalewski P. Antioxidant potential of resveratrol as the result of radiation exposition. Antioxidants. 2022;11(11). doi:10.3390/antiox11112097.

5. Bejenaru LE, Biţă A, Belu I, et al. Resveratrol: a review on the biological activity and applications. Appl Sci. 2024;14(11). doi:10.3390/app14114534.

6. Cui Q, Wang H. Resveratrol in dermatological therapy: a critical review of mechanisms, delivery innovations, and clinical frontiers. Clin Cosmet Investig Dermatol. 2025;18:2229-2242. doi:10.2147/CCID.S543849.

7. Buya AB, Beloqui A, Memvanga PB, Préat V. Self-nano-emulsifying drug-delivery systems: from development to current applications and challenges in oral drug delivery. Pharmaceutics. 2020;12(12):1-52. doi:10.3390/pharmaceutics12121194.

8. Morakul B, Teeranachaideekul V, Limwikrant W, Junyaprasert VB. Dissolution and antioxidant potential of apigenin self nanoemulsifying drug delivery system for oral delivery. Sci Rep. 2024;14(1). doi:10.1038/s41598-024-59617-z.

9. Thorsteinsdóttir UA, Thorsteinsdóttir M. Design of experiments for development and optimization of a liquid chromatography coupled to tandem mass spectrometry bioanalytical assay. J Mass Spectrom. 2021;56(9). doi:10.1002/jms.4727.

10. Yen CC, Chang CW, Hsu MC, Wu YT. Self-nanoemulsifying drug delivery system for resveratrol: enhanced oral bioavailability and reduced physical fatigue in rats. Int J Mol Sci. 2017;18(9). doi:10.3390/ijms18091853.

11. Balata GF, Essa EA, Shamardl HA, Zaidan SH, Abourehab MAS. Self-emulsifying drug delivery systems as a tool to improve solubility and bioavailability of resveratrol. Drug Des Devel Ther. 2016;10:117-128. doi:10.2147/DDDT.S95905.

12. Suwarmi, Suwaldi, Martien R, Riyanto S. Formulation and optimization of cremophore and PEG 400 in self nanoemulsifying drug delivery system resveratrol with soybean oil as a carrier. AIP Conf Proc. 2023;2706. doi:10.1063/5.0120389.

13. Sharma B, Iqbal B, Kumar S, Ali J, Baboota S. Resveratrol-loaded nanoemulsion gel system to ameliorate UV-induced oxidative skin damage: from in vitro to in vivo investigation of antioxidant activity enhancement. Arch Dermatol Res. 2019;311(10):773-793. doi:10.1007/s00403-019-01964-3.

14. Zingale E, Bonaccorso A, D'Amico AG, et al. Formulating resveratrol and melatonin self-nanoemulsifying drug delivery systems for ocular administration using design of experiments. Pharmaceutics. 2024;16(1). doi:10.3390/pharmaceutics16010125.

15. Nandiyanto ABD, Ragadhita R, Fiandini M. Interpretation of Fourier transform infrared spectra: a practical approach in polymer/plastic thermal decomposition. Indones J Sci Technol. 2023;8(1):113-126. doi:10.17509/ijost.v8i1.53297.

16. Pathade P, Sumrao A, Sonawane B, et al. Development and validation of stability indicating UV spectrophotometric method for estimation of resveratrol in bulk and tablet dosage form. Int J Drug Deliv Technol. 2024;14(1):385-388. doi:10.25258/ijddt.14.1.56.

17. International Council for Harmonisation of Technical Requirements for Pharmaceuticals for Human Use. ICH Q2(R2): Guideline on validation of analytical procedures. European Medicines Agency; 2023.

18. Rehman FU, Farid A, Shah SU, et al. Self-emulsifying drug delivery systems: measuring energy dynamics to determine thermodynamic and kinetic stability. Pharmaceuticals. 2022;15(9). doi:10.3390/ph15091064.

19. Sabrina LM, Zahra AA, Aini KN, Maulida VS, Putra HE. Comparative analysis of surfactants and cosurfactants and physical parameters in herbal-based SNEDDS formulations. J Ilm Respati. 2025;16(1):63-74. doi:10.52643/jir.v16i1.5432.

20. Muhtadi WK, Firmansyah F, Agustini TT, et al. Development, characterization, and in vitro dissolution of SNEDDS for effective oral delivery of quercetin. J Res Pharm. 2022;26(7):1937-1945. doi:10.29228/jrp.287.

21. Setiani I, Endriyatno NC. Formulation of tomato fruit extract gel with variations in HPMC concentration and physical evaluation. Indones J Pharm Educ. 2023;3(3). doi:10.37311/ijpe.v3i3.21186.

22. Pramita I, Yulita V, Mita N, Ramadhan AM. Effect of HPMC concentration as a gelling agent with a humectant combination on the physical characteristics of gel bases. Proc 5th Mulawarman Pharm Conf. 2017.

23. Al-Suwayeh SA, Badran MM, Alhumoud GO, et al. Design and dermatokinetic appraisal of lornoxicam-loaded ultrafine self-nanoemulsion hydrogel: in vitro and in vivo studies. Saudi Pharm J. 2023;31(6):889-903. doi:10.1016/j.jsps.2023.04.004.

24. Constantinescu T, Mihis AG. Resveratrol as a privileged molecule with antioxidant activity. Food Chem Adv. 2023;3:100539. doi:10.1016/j.focha.2023.100539.

25. Erwin E, Pusparohmana WR, Sari IP, Hairani R, Usman U. GC-MS profiling and DPPH radical scavenging activity of the bark of Tampoi. F1000Research. 2019;7:1977. doi:10.12688/f1000research.16643.2.

26. Jannah SRN, Zubaydah WOS, Idrus LS, Malina R, Jaya MRJ. Penetration of diclofenac sodium transfersome gel in Wistar rat skin using a Franz diffusion cell. J Mandala Pharmacon Indones. 2024;10(2):656-663. doi:10.35311/jmpi.v10i2.672.

27. Mappamasing F, Anwar E, Mun'im A. Formulation, characterization and in vitro penetration study of resveratrol solid lipid nanoparticles in topical cream. J Ilmu Kefarmasian Indones. 2015;13(2):137-144.

28. Malge TG, Game MD. Isobestic method for simultaneous estimation of resveratrol and quercetin. Int J Adv Res Sci Commun Technol. 2022;2(8). doi:10.48175/568.

29. Nandita SP, Kuncahyo I, Harjanti R. Formulation and optimization of furosemide SNEDDS with variation in Tween 80 and PEG 400 concentrations. J Fundam Appl Pharm Sci. 2021;2(1):34-42. doi:10.18196/jfaps.v2i1.12180.

30. Sari DEM, Yudanti GP, Fitrianingsih S, Hidayati R, Zahro DF. Variation of guar gum and Carbopol 940 as gelling agents on the physical and chemical properties of salak fruit extract gel. Cendekia J Pharm. 2024;8(1):71-87. doi:10.31596/cjp.v8i1.268.

31. Argenziano M, Ansari IA, Muntoni E, Spagnolo R, Scomparin A, Cavalli R. Lipid-coated nanocrystals as a tool for improving the antioxidant activity of resveratrol. Antioxidants. 2022;11(5). doi:10.3390/antiox11051007.

**32.** Vega MJ, Moreno-Fernández S, Pontes-Quero GM, et al. Characterization of novel synthetic polyphenols: validation of antioxidant and vasculoprotective activities. Antioxidants. 2020;9(9):787. doi:10.3390/antiox9090787.